

fects on  $c_s$  for low doping, I can also estimate  $E_b$  for the doping levels 13.5% and 10%.

Using the value from (13), I obtain  $\lambda_c = 3 \pm 1 \mu\text{m}$  for optimal doping, which is embarrassingly close. The agreement between the measured and estimated values of  $\lambda_c$  (Fig. 3) both as to numerical value and trend is heartening. For 214, driving a critical Josephson current is precisely sufficient to erase the energy of the superconducting correlation. Undoubtedly, it is possible to invent a system of carefully balanced cancellations that would nonetheless ascribe the source of superconductivity to internal correlations in the planes, but such logical contortions seem improbable and may even be impossible. There is no plausible intraplanar mechanism that would correlate its  $T_c$  and its energy precisely with the strength of interplanar coupling over a range of 5 to 1 in  $\lambda$ .

The case of Hg 1201 is much less airtight but still strong. Without satisfactory specific heat measurements, we are reduced to scaling the binding energy according to  $T_c^2$ , and hence,  $\lambda_c$  according to  $T_c$ . I predict, then, for Hg 1201

$$\lambda_c = 3 \mu\text{m} \times \frac{40}{90} \times \frac{d_{214}}{d_{\text{Hg}}} = 1.0 \pm 0.5 \mu\text{m} \quad (13)$$

The observed value (7) is quoted as  $1.34 \mu\text{m} \pm \sim 10\%$ . The agreement is spectacular.

The prediction for Tl 1201, on the same basis, would give  $\lambda_c \approx 0.8 \mu\text{m}$ , because  $d$  is even greater than that for Hg, but Moler *et al.* (5) find that  $\lambda_c > 15 \text{ nm}$  for the single crystals for which they have imaged vortices, and this figure is in agreement with estimates by van der Marel (3) (and with my own estimates using transport theory). This agreement is a severe anomaly. The above direct evidence for interplanar coupling in the other cases is supplemented by the neutron scattering evidence in YBCO, which shows that the gap structure is strongly correlated between planes in the close pair in just such a way as to optimize interplanar kinetic energy (10). I cannot emphasize too strongly the need to assure ourselves that Tl 1201 is genuinely a one-layer case. Some evidence for structural defects exists.

The interlayer hypothesis for the high- $T_c$  cuprates was based from the start on an experimental observation: that conductivity along the  $c$  axis is nonmetallic and incoherent, whereas that in the  $ab$  plane is metallic, if in many respects anomalous. This behavior is presumed to be a result of a non-Fermi-liquid, charge-spin-separated state; but the hypothesis can be directly tested in a manner completely independent of that conjecture. There are two experimentally testable consequences of the idea, if one is able to measure the  $c$ -axis electrostatics in the supercon-

ducting state, as has been done in a number of cases. The first is violation of the "Josephson identity", which expresses the fact that in BCS superconductors, pair tunneling replaces the coherent normal-state conduction. This violation has been noted previously by Timusk (15). The second is the requirement that the supercurrent kernel  $c/4\pi^2\lambda^2$  almost precisely match the condensation energy of the superconductors. This agreement effectively rules out any intralayer theory of high  $T_c$  and points to the interlayer concept, for those cases in which it occurs; but we are left at a loss in the one clear case where it does not.

## REFERENCES AND NOTES

1. P. W. Anderson, *The Theory of Superconductivity in the High- $T_c$  Cuprate Superconductors* (Princeton Univ. Press, Princeton, NJ, 1997).
2. ———, *Science* **268**, 1154 (1995).
3. D. van der Marel *et al.*, *Physica C* **235–40**, 1145 (1994).
4. A. J. Leggett, *Science* **274**, 587 (1996).
5. K. A. Moler, J. R. Kirtley, D. G. Hinks, T. W. Li, M. Xu, *ibid.* **279**, 1193 (1998).

6. S. Uchida, K. Tamasaku, S. Tajima, *Phys. Rev. B* **53**, 14558 (1996). Direct measurements by T. Shibauchi *et al.* [*Phys. Rev. Lett.* **72**, 2263 (1994)] agree with this more accurate method.
7. C. Panagopoulos *et al.*, *Phys. Rev. Lett.* **79**, 2320 (1997). Measurements using an untried indirect method by R. Puzniak, R. Usami, K. Isawa, and H. Yamauchi [*Phys. Rev. B* **52**, 3756 (1995)] give an implausibly short  $\lambda_c$  of  $0.43 \mu\text{m}$  and  $\xi_c \sim 2c$ , implausibly long relative to other cuprates. Theoretical and experimental uncertainties lead me to weight the Panagopoulos *et al.* value much more heavily.
8. H. F. Fong *et al.*, *Phys. Rev. Lett.* **75**, 316 (1995).
9. P. Bourges *et al.*, *Phys. Rev. B* **56**, 11439 (1997).
10. P. W. Anderson, in preparation; also in (7), p. 401; see also P. W. Anderson, *J. Phys. Chem. Solids*, in press.
11. D. H. Kim *et al.*, *Phys. Rev. Lett.* **79**, 2109 (1997).
12. A. Millis *et al.*, preprint.
13. J. W. Loram *et al.*, *Physica C* **162–4**, 498 (1989).
14. J. W. Loram, *ibid.* **235–40**, 134 (1994).
15. T. Timusk, D. N. Basov, C. C. Homes, *J. Phys. Chem. Solids* **50**, 1821 (1995). The violation is evident from the experimental infrared data, which show that the observed dc conductivity is confined to very low frequencies (statements of some experimentalists to the contrary are not consistent).
16. I should like to acknowledge extensive discussions with D. van der Marel, S. Chakravarty, D. G. Clarke, N.-P. Ong, and, especially, K. A. Moler.

4 November 1997; accepted 5 January 1998

## Communication with Chaotic Lasers

Gregory D. VanWiggeren and Rajarshi Roy\*

Recent experiments with chaotic electronic circuits have shown the possibility of communication with chaos. The experimental demonstration of chaotic communication with an optical system is described. An erbium-doped fiber ring laser (EDFRL) was used to produce chaotic light with a wavelength of 1.53 micrometers. A small 10-megahertz message was embedded in the larger chaotic carrier and transmitted to a receiver system where the message was recovered from the chaos. Chaotic optical waveforms can thus be used to communicate masked information at high bandwidths.

The demonstration of transmission and reception of information with synchronized electronic circuits (1) raised the question of optical communication with chaotic lasers. Communication with light waves with chaotic fluctuations of intensity has been considered in recent years by several investigators (2). The natural masking of information by chaotic fluctuations has served as a practical motivation for the research. Great interest also exists in understanding the basic mechanisms by which information can be encoded and decoded through the use of synchronized chaotic systems.

Although chaotic communication experiments with electronic circuits (1) have typically demonstrated information transmission at bandwidths of tens of kilohertz or

less, the fast dynamics often displayed by optical systems offers the possibility of communication at bandwidths of hundreds of megahertz or higher. In the past few years, we have explored the fast dynamics of erbium-doped fiber ring lasers (EDFRLs) (3) with the goal of achieving optical communication with chaotic lasers. These lasers are particularly well suited for communication purposes because their lasing wavelengths roughly correspond to the minimum-loss wavelength in optical fiber. Such fiber ring lasers are capable of displaying both low- ( $\leq 3$ ) and high-dimensional ( $> 3$ ) dynamics under different conditions of operation. We report optical experiments that demonstrate message transmission and reception at 10 MHz with a chaotic carrier at  $\sim 1.53 \mu\text{m}$ .

The output beam from an external cavity, tunable semiconductor laser is amplitude modulated with a 10-MHz square wave (the "message") by a lithium niobate Mach-Zehnder modulator (Fig. 1). The message is

School of Physics, Georgia Institute of Technology, Atlanta, GA 30332, USA.

\*To whom correspondence should be addressed. E-mail: rajarshi.roy@physics.gatech.edu

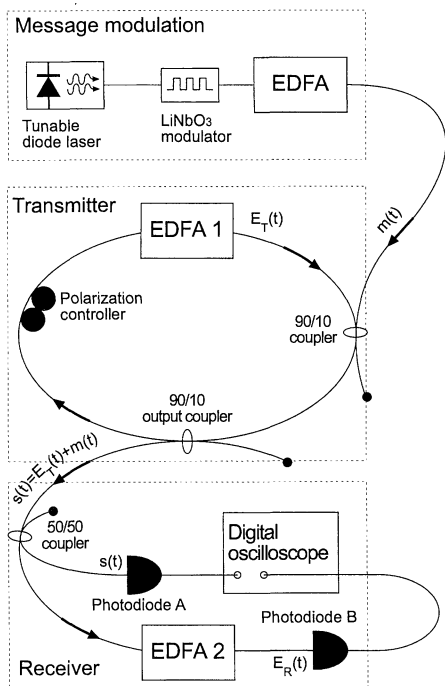


**Fig. 1.** Experimental system for optical communication with chaotic lasers. A coupler injects the modulated semiconductor laser signal with the message into the fiber ring laser. The output of the transmitter is extracted through another coupler and directed to the receiver EDFA 2 and photodiode A by a 50/50 coupler. The receiver input and output are detected by the photodiodes A and B. The photodiode signals are recorded on the digital oscilloscope and processed to recover the message.

amplified by an erbium-doped fiber amplifier (EDFA) in the message modulation unit before injection into the ring laser transmitter. This operation allows us to adjust the proportion of message to chaotic carrier in the transmitter EDFRL. The message is then injected into the EDFRL through a 90/10 waveguide coupler. The notation indicates that 10% of the message is injected into the ring and 90% of the light within the ring is retained. The semiconductor laser wavelength (1.5328  $\mu\text{m}$ ) is tuned to resonance with one of the two peaks of the EDFA gain spectrum. The transmitter output is extracted with another 90/10 coupler. In our setup, an optical fiber a few meters long connects the transmitter to the receiver. In a real system, a much longer fiber could be used.

A 50/50 coupler divides the output between photodiode A and EDFA 2 in the receiver. EDFA 2 has been fabricated to match EDFA 1 as closely as possible—their pump diode laser and active medium fiber length and dopant concentrations are matched carefully. The output from EDFA 2 is incident on photodiode B. The signals from the two photodiodes (125 MHz bandwidth) are recorded on the 1-GHz sampling

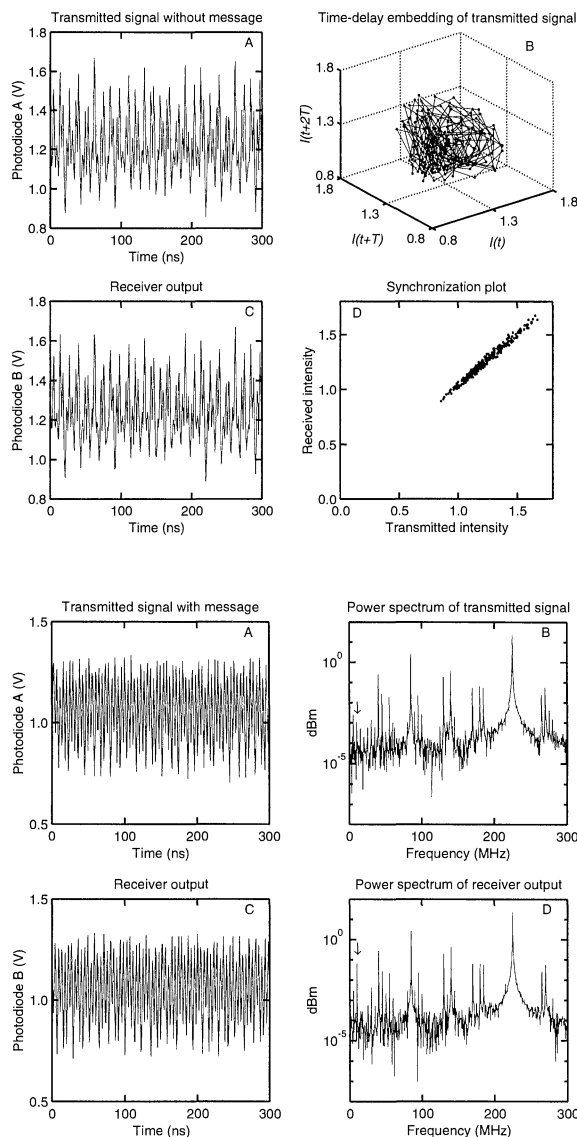


**Fig. 2.** (A) Transmitter output with no injected message. (B) Time delay embedding of the intensity time trace (A) in three dimensions with a time delay  $T = 4$  ns shows no low-dimensional structure. (C) Receiver output (delayed by  $\tau = 51$  ns) corresponding to the transmitter signal in (A). (D) Synchronization plot of the signals in (A) and (C). The input and output of the receiver are well synchronized, demonstrating that the receiver EDFA 2 tracks the transmitter laser when no message is present.

**Fig. 3.** (A) The transmitter output intensity time trace shows chaotic fluctuations. The message signal is injected into the ring laser for this recording. The message intensity is about 0.02% of the circulating intensity of the transmitter laser. (B) The power spectrum of the time trace in (A) shows a small component at the square-wave message frequency of 10 MHz indicated by the arrow. (C) The time trace of the receiver output corresponding to the transmitter trace in (A). (D) The power spectrum of the receiver output signal. An arrow indicates the 10-MHz frequency.

rate digital oscilloscope and processed as described below.

A model for the operation of the transmitter EDFRL was developed in (3) and consists of delay equations for the two orthogonally polarized components of the laser electric field in the fiber ring coupled to a differential equation for the population inversion. For the transmitter EDFRL with message injection, these equations have the form

$$\mathbf{E}_T(t) = f[\mathbf{E}_T(t - \tau_r), N(t), \mathbf{m}(t - \tau_r)] \quad (1)$$

and

$$dN(t)/dt = g[\mathbf{E}_T(t), N(t)] \quad (2)$$

where  $f$  and  $g$  are nonlinear functions of the complex field  $\mathbf{E}_T$ , which has two polarization components, and  $N$  is the population inversion;  $\mathbf{m}(t)$  represents the message field injected into the transmitter ring by the semiconductor laser, and  $\tau_r$  is the time delay that corresponds to propagation of these waves

around the fiber loop in the ring laser. From Eq. 1, the field  $\mathbf{E}_T(t)$  at the output coupler of the EDFRL depends on the field and message at the coupler one round trip earlier.

In the receiver, an open-loop technique similar to one introduced originally by Volkovskii and Rulkov (4) for electronic circuits is used to recover the message from the chaotic carrier. The transmitter signal,  $\mathbf{s}(t) = \mathbf{E}_T(t) + \mathbf{m}(t)$ , propagates from the EDFRL to photodiode A, where the signal is recorded, and to the input of the receiver. We assume for ease of explanation that the receiver system is an open-loop replica of the EDFRL; the time taken to propagate from the input of EDFA 2 to photodiode B is equal to  $\tau_r$ . The receiver EDFA operates on  $\mathbf{s}(t)$  to produce a new field,  $\mathbf{E}_R(t)$ , at photodiode B. Because the EDFAs in the transmitter and receiver are assumed to have identical functions  $f$  and  $g$  and negative conditional Lyapunov exponents, it can be shown that  $\mathbf{E}_R(t) = \mathbf{E}_T(t)$ . The

intensities at the photodiodes A and B are thus  $|E_T(t) + m(t)|^2$  and  $|E_R(t)|^2$ . The difference of these signals is  $2\text{Re}(E_T^*m) + |m(t)|^2$ . A low-pass digital filter can extract the message portion  $|m(t)|^2$  because the message is transmitted at a frequency lower than the typical frequency (hundreds of megahertz) of the chaotic carrier fluctuations. We now describe the results of our experiments.

A chaotic intensity time trace from the transmitter EDFRL without any message injection is shown in Fig. 2A. A time-delay embedding (with delay  $T = 4$  ns) of the intensity time series in Fig. 2A shows no obvious low-dimensional structure (Fig. 2B). Figure 2C shows the synchronized response from the receiver EDFA. Because the length of the passive fiber in the receiver EDFA is shorter than in the EDFRL, the signal is time shifted by the appropriate

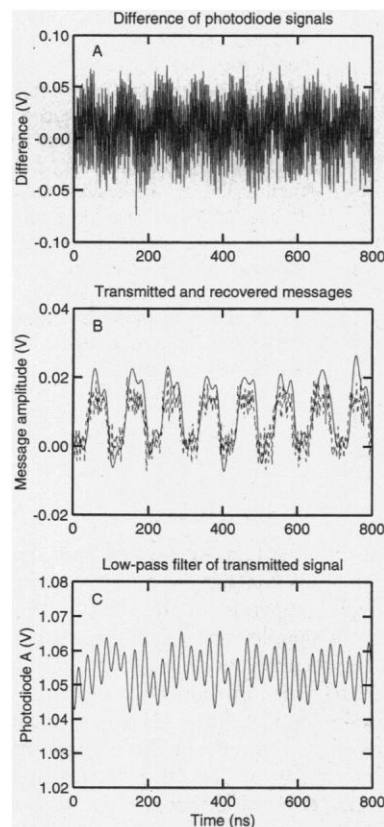


**Fig. 4.** (A) The difference of the receiver input recorded from photodiode A and receiver output recorded from photodiode B, after the transmitter signal has been shifted by the appropriate time delay  $\tau = 51$  ns. (B) The solid line is the recovered square-wave message after low-pass filtering of the difference signal in (A). The dashed line shows the message as detected by photodiode A if the transmitter EDFRL is turned off. The fluctuations are mainly due to noise from the photodiode amplifier and analog-to-digital converter in the oscilloscope. (C) Low-pass filtered version of the transmitted signal showing no trace of the square-wave message.

delay  $\tau = 51$  ns to match the trace in Fig. 2A. The time delay  $\tau$  depends on the lengths of fiber in the two branches of the receiver and on the round trip time  $\tau_r$  of the EDFRL. Figure 2D, the synchronization plot of the two signals, reveals excellent reproduction of the transmitter output by the receiver. Numerical computations and analysis of high-dimensional synchronization in a model of coupled optical ring cavities has recently been carried out by Abarbanel and Kennel (5).

A chaotic intensity time trace of the transmitter output with square-wave modulation of the injected beam is shown in Fig. 3A; Fig. 3B shows its power spectrum. The spectrum is broadband; its high-frequency components are limited by the bandwidth of the photodetector. The 20 mW of circulating power in the EDFRL is much larger than the 5  $\mu$ W of message signal injected from the message modulation unit. The square-wave fundamental frequency component is barely visible in the power spectrum of this time trace, as seen in Fig. 3B. The receiver output recorded in response to the transmitted intensity (Fig. 3A) is shown in Fig. 3C. This trace is similar, but not identical, to the transmitted signal. Its power spectrum (Fig. 3D) shows that the fundamental frequency component of the square-wave modulation and its odd harmonics have been amplified considerably (>15 dB) by the nonlinear response of the receiver EDFA; we comment below on this interesting effect.

The signals at the input and output of the receiver (recorded as time traces from photodiodes A and B) are subtracted after signal B is shifted (delayed) by  $\tau = 51$  ns, and the difference is shown in Fig. 4A. If the shift used before subtraction is incorrect, the recovered message is degraded. This difference signal is then low-pass filtered with a Butterworth filter ( $1/\sqrt{2}$  roll-off at 35 MHz), and as shown in Fig. 4B by the solid line, the masked message is recovered from the chaotic carrier fluctuations. It is easily recognized to be the square-wave modulation imposed on the injection laser. The dashed line is the message as measured directly by photodiode A when the semiconductor laser output is passed through the couplers without turning the transmitter EDFRL on. A comparison of the solid and dashed traces provides a direct measure of the receiver's ability to recover the message. The slightly greater amplitude of the recovered message can be explained by the enhancement due to the nonlinear response of the receiver EDFA discussed below. For comparison, the same low-pass filter as above has been applied to the transmitted signal in Fig. 3A, and the result is shown in Fig. 4C. The 200-ns periodicity corresponds

to the round-trip time of the laser; the square-wave message is not visible in this trace.

The EDFAs in both the transmitter and receiver are operated at high pump powers for which saturation nonlinearities are important. The receiver has the same nonlinearities as the transmitter, allowing it to unfold the message from the chaos. Comparison of Fig. 3B with Fig. 3D shows that these inherent nonlinearities also allow the receiver EDFA to amplify preferentially the frequency components of the message signal. This preferential amplification permits the recovery of messages with smaller amplitudes than would be possible otherwise. Indeed, the recovered message has a slightly larger amplitude than the directly detected message (Fig. 4B). These observations of preferential amplification are reminiscent of the phenomena of stochastic or chaotic resonance (6), which have been studied during the past decade in nonlinear systems driven simultaneously by periodic signals and noise. There are no intrinsic restrictions on optical communication at much higher rates than demonstrated here, particularly if a direct subtraction of the electric fields at the input and output of the receiver is performed by an optical heterodyne technique.

## REFERENCES AND NOTES

1. L. M. Pecora and T. L. Carroll, *Phys. Rev. A* **44**, 2374 (1991); W. L. Ditto and L. M. Pecora, *Sci. Am.* **269**, 62 (August 1993); K. M. Cuomo and A. V. Oppenheim, *Phys. Rev. Lett.* **71**, 65 (1993); S. H. Strogatz, *IEEE Trans. Circuits Syst.* **40**, 626 (1993); L. Kocarev, K. S. Halle, K. Eckert, L. O. Chua, U. Parlitz, *Int. J. Bifur. Chaos Appl. Sci. Eng.* **2**, 709 (1992); U. Parlitz, L. Kocarev, T. Stojanovski, H. Preckel, *Phys. Rev. E* **53**, 4351 (1996).
2. R. Roy and K. S. Thornburg Jr., *Phys. Rev. Lett.* **72**, 2009 (1994); T. Sugawara *et al.*, *ibid.*, p. 3502; P. Colet and R. Roy, *Opt. Lett.* **19**, 2056 (1994); C. R. Mirasso, P. Colet, P. Garcia-Fernandez, *IEEE Phot. Tech. Lett.* **8**, 299 (1996); P. M. Alsing, A. Gavrielides, V. Kovanic, R. Roy, K. S. Thornburg Jr., *Phys. Rev. E* **56**, 6302 (1997).
3. Q. L. Williams and R. Roy, *Opt. Lett.* **21**, 1478 (1996); Q. L. Williams, J. Garcia-Ojalvo, R. Roy, *Phys. Rev. A* **55**, 2376 (1997); J. Garcia-Ojalvo and R. Roy, *Phys. Lett. A* **229**, 362 (1997).
4. A. R. Volkovskii and N. Rulkov, *Tech. Phys. Lett.* **19**, 97 (1993).
5. H. D. I. Abarbanel and M. Kennel, *Phys. Rev. Lett.*, in press.
6. B. McNamara, K. Wiesenfeld, R. Roy, *Phys. Rev. Lett.* **60**, 2626 (1988); K. Wiesenfeld and F. Moss, *Nature* **373**, 33 (1995).
7. We thank H. Abarbanel, M. Kennel, M. Lanzerotti, L. Larger, P. O'Shea, U. Parlitz, L. Pecora, N. Rahaghi, N. Rulkov, S. Strogatz, S. Thornburg, K. Wiesenfeld, and S. Yeung for helpful discussions. C. Verber, P. Juodawlkis, and M. Gross provided essential instrumentation and encouragement. Support from the National Science Foundation (grant NCR 961225) and the Office of Naval Research is gratefully acknowledged.

11 November 1997; accepted 12 January 1998